

VEP contrast sensitivity responses reveal reduced functional segregation of mid and high filters of visual channels in Autism

Boutheina Jemel

Research Laboratory in Neuroscience and Cognitive Electrophysiology, Hôpital Rivière des Prairies, Université de Montréal, Montreal, Canada



Daniel Mimeault

Hôpital Rivière des Prairies, Clinique Spécialisée de l'Autisme, Montreal, Canada



Dave Saint-Amour

CHU Sainte Justine Research Center, Department of Ophthalmology, Université de Montréal, Montreal, Canada



Anthony Hosein

Research Laboratory in Neuroscience and Cognitive Electrophysiology, Hôpital Rivière des Prairies, Montreal, Canada



Laurent Mottron

Centre d'excellence en Troubles envahissants du développement, Hôpital Rivière-des-Prairies, Université de Montréal, Montréal, Canada



Despite the vast amount of behavioral data showing a pronounced tendency in individuals with autism spectrum disorder (ASD) to process fine visual details, much less is known about the neurophysiological characteristics of spatial vision in ASD. Here, we address this issue by assessing the contrast sensitivity response properties of the early visual-evoked potentials (VEPs) to sine-wave gratings of low, medium and high spatial frequencies in adults with ASD and in an age- and IQ-matched control group. Our results show that while VEP contrast responses to low and high spatial frequency gratings did not differ between ASD and controls, early VEPs to mid spatial frequency gratings exhibited similar response characteristics as those to high spatial frequency gratings in ASD. Our findings show evidence for an altered functional segregation of early visual channels, especially those responsible for processing mid- and high-frequency spatial scales.

Keywords: autism spectrum disorder, contrast sensitivity, visual evoked potentials, spatial vision

Citation: Jemel, B., Mimeault, D., Saint-Amour, D., Hosein, A., & Mottron, L. (2010). VEP contrast sensitivity responses reveal reduced functional segregation of mid and high filters of visual channels in Autism. *Journal of Vision*, 10(6):13, 1–13, <http://www.journalofvision.org/content/10/6/13>, doi:10.1167/10.6.13.

Introduction

Autism spectrum disorder (ASD) is mostly known as a neurogenetic developmental variant, characterized by qualitative and/or quantitative disabilities in social interaction and communication as well as restricted interests and activities (American Psychiatric Association, 2000; Volkmar, Lord, Bailey, Schultz, & Klin, 2004). Its phenotypes comprise autistic disorder (AD) with or without intellectual disability as well as Asperger syndrome (AS).

Besides the mainstream line of research investigating clinically tagged social disabilities in autism (cf. Jemel, Mottron, & Dawson, 2006), the breadth of recent behavioral and neuroimaging studies has rather focused on the islets of abilities in this condition. Convergent evidence

has established that visual processing in ASD is both enhanced and locally oriented as compared to typically developing individuals (Dakin & Frith, 2005; Happé, 1999; Mottron, Dawson, Soulieres, Hubert, & Burack, 2006). ASD individuals outperform non-autistic individuals in various tasks that involve detection of local visual elements embedded in large figures, such as the block design task (Caron, Mottron, Berthiaume, & Dawson, 2006; Shah & Frith, 1993), the embedded figures task (Jolliffe & Baron-Cohen, 1997; Shah & Frith, 1983), the Navon-type tasks (Rinehart, Bradshaw, Moss, Brereton, & Tonge, 2000; Wang, Mottron, Peng, Berthiaume, & Dawson, 2007), and feature-conjunction search tasks (O'Riordan & Plaisted, 2001). These findings led several authors to conclude that the superiority of people with ASD to visually resolve small objects in large displays results from a dysfunction (Dakin & Frith, 2005) or an

over-functioning (Mottron et al., 2006) of spatial filter channels in the early visual system.

In human spatial vision, research in visual neuroscience and psychophysics has shown that the first processing steps in visual scene analysis implicate an array of six linear visual filters, or channels, each of which is sensitive to narrow ranges of spatial frequencies and displays a specific contrast–tuning curve (Campbell & Robson, 1968; Dacey & Petersen, 1992; DeValois & DeValois, 1988; Nassi & Callaway, 2009; Pantle & Sekuler, 1968; Shapley, 1990; Wilson, McFarlane, & Phillips, 1983; Wilson & Wilkinson, 2004). The spatial performance of these visual channels can be assessed in human observers through the psychophysical measurement of contrast sensitivity functions or CSF (Campbell & Green, 1965; Campbell & Robson, 1968). Previous studies have revealed that CSFs vary between individuals as a function of age (Movson & Kiorpes, 1988; Sekuler & Hutman, 1980) or pathological conditions (Bulens, Meerwaldt, van der Wildt, & Keemink, 1988; McKee, Levi, & Movshon, 2003), and this variation is caused by differences in the relative sensitivity of the underlying neural channels in the early visual cortical processing streams.

Furthermore, pattern detection capabilities of the visual system can be non-invasively characterized using scalp recordings of visual-evoked potentials (VEPs). It is generally accepted that VEPs provide an objective evaluation of visual resolution and contrast sensitivity in human adults and infants (Fiorentini, Pirchio, & Spinelli, 1980; Norcia & Tyler, 1985; Regan, 1989) and the integrity of cortical visual channels in several clinical conditions (Butler et al., 2007). Previous research investigating transient VEPs to contrast reversal gratings has demonstrated that VEP amplitude versus contrast functions vary as a function of spatial frequency and thus reflect the activity of spatial-specific processing channels within the visual cortex (Baseler & Sutter, 1997; Ellemberg, Hammarranger, Lepore, Roy, & Guillemot, 2001; Klistorner, Crewther, & Crewther, 1997; Nelson & Seiple, 1992; Plant, Zimmern, & Durden, 1983; Regan, 1989; Rudvin, Valberg, & Kilavik, 2000; Souza, Gomes, Saito, da Silva Filho, & Silveira, 2007; Vassilev, Stomonyakov, & Manahilov, 1994). More specifically, it was found that at low spatial frequencies, the contrast–response curve of P100 VEP peak is characterized by a non-linear saturating response–contrast function (Baseler & Sutter, 1997; Ellemberg et al., 2001; Klistorner et al., 1997; Souza et al., 2007). As the contrast level is increased, P100 amplitude gradually increases and rapidly saturates at fairly low contrasts. Furthermore, the VEPs at intermediate and high spatial frequency gratings enclose two consecutive peaks (i.e., N80 and P100 peaks), the amplitudes of which increase linearly with contrast, and do not tend to level off (Bach & Ullrich, 1997; Ellemberg et al., 2001; Vassilev et al., 1994). The response versus contrast function of these peaks thus displays a straight line up to the highest contrasts (Bach & Ullrich, 1997; Ellemberg et al., 2001; Souza et al., 2007).

In autism, studies investigating spatial vision in children and adults with ASD have nevertheless produced mixed results (Behrmann et al., 2006; Bertone, Mottron, Jelenic, & Faubert, 2005; Boeschoten, Kenemans, van Engeland, & Kemner, 2007a; Davis, Bockbrader, Murphy, Hetrick, & O'Donnell, 2006; De Jonge et al., 2007; McCleery, Allman, Carver, & Dobkins, 2007; Milne, Scope, Pascalis, Buckley, & Makeig, 2009). While some studies did not find any difference in contrast sensitivity thresholds between ASD individuals and their matched controls (Behrmann et al., 2006; Bertone et al., 2005; de Jonge et al., 2007), findings from other studies indicate an atypical functioning of the visual channels responsible for processing low but also high spatial frequency information (Boeschoten et al., 2007a; Davis et al., 2006; McCleery et al., 2007; Milne et al., 2009). Luminance contrast sensitivity thresholds were found to be either reduced for high spatial frequency gratings (13.4 c-deg^{-1}) in children with autism (Davis et al., 2006) or enhanced for 0.27 c-deg^{-1} spatial frequency gratings in high-risk 6-month-old infants, whose older siblings were diagnosed with ASD (McCleery et al., 2007). In addition, findings from two recent electrophysiological studies indicate reduced response tuning of cortical responses to spatial frequency information in children with autism (Boeschoten et al., 2007a; Milne et al., 2009). More specifically, these studies found that unlike control participants, children with ASD show decreased differentiation of cortical visual responses to different spatial frequency patterns. It is worth noting, however, that in these two studies (Boeschoten et al., 2007a; Milne et al., 2009), the various spatial frequency patterns used were presented at a fixed high contrast level, a manipulation that does not allow a thorough investigation of the response dynamics of cortical visual channels in autism.

In the present study, we sought to further assess early spatial vision in autism using transient VEP recordings to contrast–luminance changes of sine-wave gratings with different spatial frequencies (SF). Among the six SF grating conditions tested in the study of Ellemberg et al. (2001), we have chosen three specific spatial frequency bands, i.e., low (0.8 c-deg^{-1}), mid (2.8 c-deg^{-1}), and high (8 c-deg^{-1}), which have been shown to elicit distinct VEP contrast response profiles. The evaluation of the VEP contrast–response tuning curves allowed us to characterize the functional properties of low, mid, and high spatial visual channels in a group of young adults with autism as compared to an age- and IQ-matched group of typically developing individuals.

Methods

Participants

Participants were 18 young adults meeting DSM-IV-TR criteria (APA, 2000) for “autistic disorder” (15 males,

	AD, Mean \pm SD (range)	Asperger, Mean \pm SD (range)	Control, Mean \pm SD (range)
Gender (M/F)	8/0	6/2	13/1
Age (years)	25.5 \pm 4.6 (18–31)	25.8 \pm 4.5 (18–31)	25 \pm 5.1 (20–33)
Full scale IQ	105 \pm 13.8 (87–118)	97.8 \pm 10.8 (84–113)	104.1 \pm 10.1 (87–121)
Verbal IQ	105.4 \pm 15.7 (81–121)	101 \pm 8.8 (88–114)	108.2 \pm 10.1 (94–127)
Performance IQ	102.5 \pm 11.4 (80–116)	97.1 \pm 11.2 (84–109)	101.2 \pm 15.4 (79–127)

Table 1. Mean age and IQ scores for ASD (8 participants with autism AD and 8 participants with Asperger) and control participants.

2 females) and 15 typically developing controls (14 males, 1 female). Data of one control and two ASD participants were excluded from analyses due to excessive noise in the EEG data, thus leaving a total of 16 ASD and 14 controls. As summarized in Table 1, all ASD participants were of typical intelligence levels (FS-IQ > 80), and they were matched as closely as possible to control participants with respect to gender, chronological age, and IQ as assessed by the Wechsler Adult Intelligence Scale III (Wechsler, 1997).

Participants with ASD were recruited from the Autism Specialized Clinic (Rivière-des-Prairies Hospital, Montreal). Diagnoses were based on the Autism Diagnostic Interview-Revised (ADI-R; Lord, Rutter, & Le Couteur, 1994) and/or the Autism Diagnostic Observation Schedule (ADOS; Lord et al., 2000). Among the ASD group, 8 participants received a specific diagnosis of autistic disorder (AD), and the remainder ($n = 8$) received a specific diagnosis of Asperger syndrome based on information from the ADI-R, indicating the absence of speech delay, echolalia, pronoun reversal, or evident stereotyped language. Table 2 provides descriptive clinical information for the two ASD subgroups.

All ASD participants were screened for additional psychiatric and neurological diagnoses and were free from medication. Typically developing control participants were recruited from a panel maintained by the same institution and screened for history of autism or other psychiatric conditions in themselves and in their first-degree relatives. All participants had normal or corrected to normal vision. Informed consent was obtained from each participant after

the nature of the study was explained, in accordance with the regulations of the ethical committee of Rivière-des-Prairies Hospital.

Stimuli and design

Stimuli were vertical sinusoidal achromatic gratings of low (LSF: 0.8 c·deg⁻¹), mid (MSF: 2.8 c·deg⁻¹), and high spatial frequencies (HSF: 8 c·deg⁻¹), all windowed by a Gaussian envelope. The contrast of each SF grating, calculated as $C = 100 \times (L_{\max} - L_{\min}) / (L_{\max} + L_{\min})$, where L_{\max} = luminance of the bright stripes and L_{\min} = luminance of the dark stripes (Michelson, 1927), took one of four different values: 4%, 8%, 32%, or 90%. Stimuli were generated by a PC-4 computer using Presentation software and displayed on a Philips LightFrame 109B55 monitor (1280 \times 1024, 90 Hz). The phase of each grating was reversed at a fixed temporal rate of 2 Hz (four reversals per second). The luminance of the monitor was gamma corrected, and both the calibration and luminance readings were regularly verified using a CS-100 Chroma Meter.

Participants were seated inside a dimly lit and electrically shielded room and instructed to fixate binocularly the center of the display (15 \times 15 deg) at a viewing distance of 57 cm. They were asked to detect a rare target stimulus (a horizontal grating on 5% of the trials) by pressing on a mouse key button as accurately and as rapidly as possible. Each of the spatial frequency by contrast reversing grating

	AD, Mean \pm SD (range)	Asperger, Mean \pm SD (range)
ADI-R	$n = 8$	$n = 7$
Social (10)	24 \pm 5.3 (15–29)	22.1 \pm 5.9 (10–27)
Communication (8)	16.6 \pm 4.1 (10–22)	15.9 \pm 2.9 (14–21)
RIRB (3)	7.9 \pm 1.7 (5–10)	6.6 \pm 2.7 (3–12)
ADOS	$n = 6$	$n = 8$
Social (7)	10 \pm 1.7 (8–12)	10.6 \pm 1.6 (8–13)
Communication (4)	6 \pm 1.7 (4–9)	5.8 \pm 1.5 (3–8)
RIRB (no cutoff)	3 \pm 2.1 (0–5)	3.1 \pm 1.7 (0–6)

Table 2. All ASD participants (AD and Asperger) had a score above the ADI/ADOS cutoffs for autism diagnosis in the three relevant areas: social domain, communication domain, and restricted interest/repetitive behavior (RIRB). The autism cutoff scores are indicated in parentheses.

conditions (3 SF \times 4 contrasts) was presented for a total of 104 trials. The order of presentation was randomized in order to avoid any effects of habituation and/or fatigue.

EEG recording and VEP analysis

The electroencephalogram (EEG) was recorded with 58 electrically shielded Ag/AgCl electrodes embedded in an elastic Easy cap according to the enhanced 10–20 system (Sharbrough et al., 1991). Two additional bipolar electrodes placed above and below the dominant eye (vertical EOG) and at the outer canthus of each eye (horizontal EOG) were used to monitor eye blinks and horizontal eye movements. A left earlobe electrode was used as a reference for all electrodes. Electrode impedances were always kept below 5 k Ω . The EEG and the EOG were recorded continuously with a band-pass from DC to 100 Hz at a sampling rate of 1024 Hz and stored along with the trigger codes.

The EEG signal was off-line filtered using a digital band-pass filter (0.03–30 Hz) and re-referenced using an average reference (Nunez, 1981). EEG segments with eye blinks and other artifacts were automatically rejected (i) if the standard deviation of the EOG channels within a 200-ms sliding window exceeds 40 μ V and (ii) if the standard deviation of any scalp electrode exceeds 20 μ V. Eye blinks were then detected and corrected by subtracting from the EEG the PCA-transformed EOG components for each electrode, weighted according VEOG propagation factors (computed via linear regression). Artifact-free EEG segments time locked to the onset of the gratings synchronized with the “on-contrast” phase were averaged from 50 ms before and 300 ms after stimulus onset separately for each frequency and contrast grating. Baselines were computed in the interval from 50 to 0 ms prior to stimulus onset and subtracted before averaging. Across all conditions, the mean number of artifact-free trials included for VEP averaging did not differ between the two groups; 85.4 (range = 34–104) and 87.3 (range = 55–103), respectively, for ASD and controls (independent samples *t*-test (28) < 1.15; *p* > 0.3, for all spatial frequency by contrast conditions).

After averaging, peak amplitude and latency measures of the early VEP components were quantified within specific time-windows over the midline occipital scalp electrode Oz. The N80 VEP component was defined as the largest negative peak between 70 and 110 ms and the P100 as the largest positive peak between 90 and 140 ms.

The contrast sensitivity response of P100 and N80 VEP peaks for ASD and control groups were assessed separately for each SF condition, using the non-linear and linear curve fitting procedures provided by statistical analysis software (Sigmaplot 2D; Systat Software, Inc., Point Richmond, CA). Non-linearities in the function relating the amplitude of P100 evoked by LSF gratings and the Michaelson contrast *C* were fitted to the Michaelis–

Menten equation as applied to visual physiology (Naka & Rushton, 1966; Shapley & Enroth-Cugell, 1984). The equation is:

$$R = R_{\max} \times C^n / (b + C^n), \quad (1)$$

where *R* is VEP response amplitude, R_{\max} represents the derived maximum value of VEP amplitude, *b* represents the derived semi-saturation contrast, that is the contrast level eliciting half the maximal VEP amplitude response ($R_{\max}/2$), and the exponent *n* is a measure of the steepness of the curve (response exponent). Linear models of the form, $R = a + b \times x$, were used to fit N80 and P100 contrast responses to MSF and HSF gratings. To assess possible group differences in the functions relating VEP responses to contrast luminance gratings, linear and non-linear functions were applied to individual data. The values of the estimated parameters of these fits, i.e., half saturation (*b*) and response saturation (R_{\max}) values derived from the Naka–Rushton function and the slope (*b*) of linear functions, were then compared between groups using independent samples *t*-tests and between spatial frequency conditions using paired sample *t*-tests. Additional statistical analyses were performed on P100 and N80 peak latency and amplitude measures using repeated measures analyses of variance (ANOVAs) with appropriate Greenhouse–Geisser corrections, with ASD and control groups as between-participants factor and spatial frequency grating condition (LSF, MSF, HSF for P100 measures, and MSF and HSF only for N80 measures) and contrast level (4%, 8%, 32%, and 90%) as within-participants factors.

Results

Electrophysiological results

Figure 1 depicts the major transient VEP peaks recorded over the occipital Oz electrode in response to low, medium, and high spatial frequency of luminance-contrast gratings (i.e., 4%, 8%, 32%, and 90%) separately in the ASD (Figure 1A) and control group (Figure 1B). These VEPs enclose an initial negative-going deflection (N80) peaking around 70 and 90 ms in response to MSF and HSF grating conditions only, and a positive deflection (P100) peaking around 110 and 130 ms visible for the three spatial frequency conditions (LSF, MSF, HSF). The 3-D scalp maps displayed in Figure 1 show a clear midline occipital distribution of the N80 and P100 peaks.

In agreement with previous reports (Bach & Ullrich, 1997; Baseler & Sutter, 1997; Elleberg et al., 2001), the amplitude variations of these VEPs to luminance-contrast gratings were differentially modulated by spatial frequency conditions in both ASD and control groups. In addition, the spatial scale and contrast of gratings also modulated

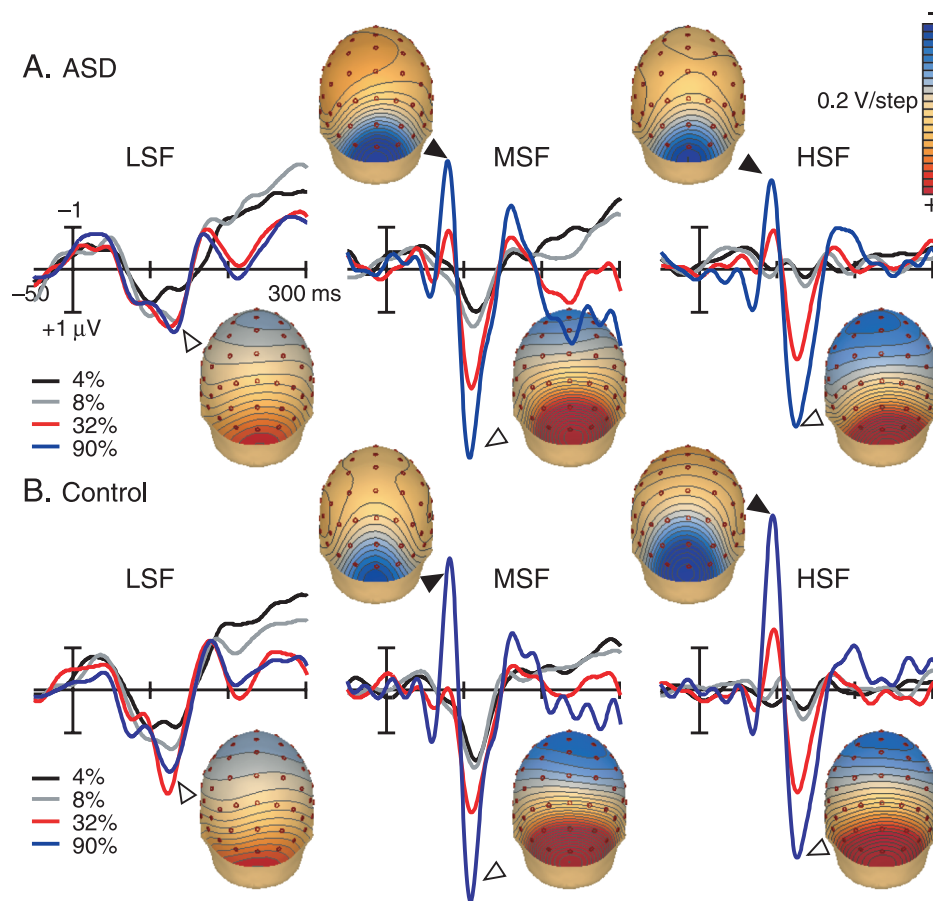


Figure 1. Grand-average VEPs for LSF, MSF, and HSF gratings in the ASD (A) and control group (B). Superimposed are the VEP waveforms at 4%, 8%, 32%, and 90% contrast levels of each spatial frequency grating. Data are from the midline occipital electrode Oz. Scalp topographical distribution of the P100 (open arrow) and N80 (filled black arrow) responses are shown for each spatial frequency grating at 90% contrast.

the latency of these VEP peaks (Mihaylova, Stomonyakov, & Vassilev, 1999; Vassilev, Mihaylova, & Bonnet, 2002). More specifically, N80 latency increased both on increasing grating spatial frequency and on reducing grating contrast. This pattern of N80 latency increase did not differ between ASD and controls (spatial frequency by contrast by group interaction: $F < 2.3$, $p > 0.08$).

N80 contrast sensitivity functions

As shown in Figure 1, the contrast dependence of N80 amplitudes was virtually identical in both groups; N80 elicited by MSF and HSF gratings was smaller at low contrast levels and linearly increased as the contrast luminance increased for both ASD and control groups. However, the pattern of N80 contrast response changes was slightly different for MSF and HSF gratings and between ASD and controls. This was confirmed by a significant high-level interaction involving spatial frequency, contrast, and group factors ($F(2.3, 64.4) = 3.92$,

$\varepsilon = 0.77$, $p = 0.02$). This interaction indicated two main results.

First, while controls showed larger N80 amplitudes to HSF than to MSF gratings across all contrast levels (except for the 4% contrast), no such N80 modulations were found in ASD. Second, N80 contrast responses displayed distinct behaviors in response to MSF and HSF grating in controls, whereas similar N80 contrast responses to spatial frequency grating were noted in ASD. More specifically, controls show conspicuous N80 peaks that were elicited at 90% contrast for MSF gratings and at 32% and 90% contrasts for HSF gratings. Conversely, N80 peaks in ASD were clearly visible at 32% and 90% contrasts for both MSF and HSF gratings. These latter results indicate that early N80 cortical response triggered by MSF and HSF gratings exhibits distinct contrast patterns in controls, but their contrast sensitivities were similar in ASD.

To further qualify the pattern of N80 amplitude modulations by contrast–luminance gratings in each group of participants, we assessed the slope of the N80 contrast

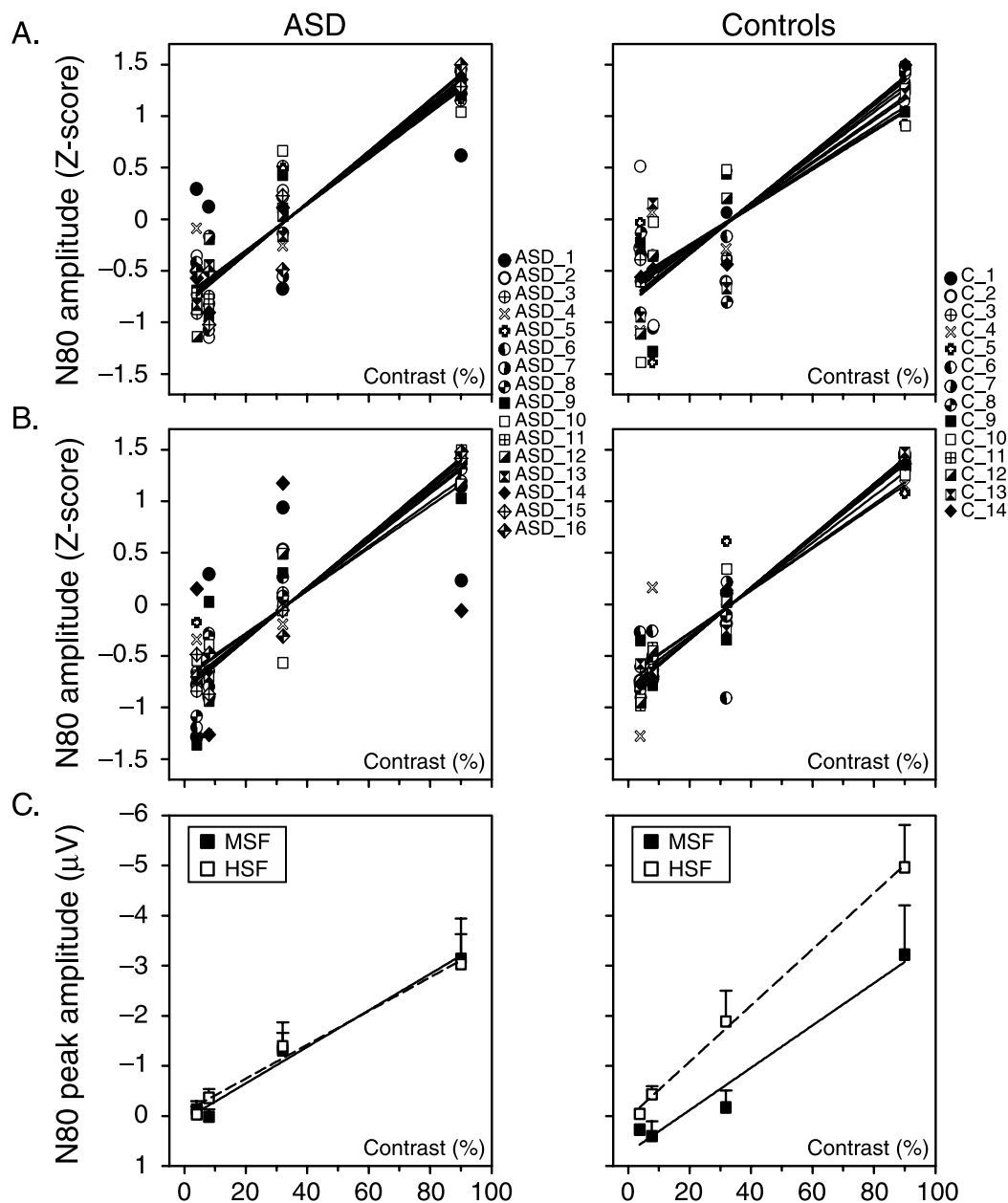


Figure 2. Best fitting curves of contrast responses of N80 peaks computed for each individual data of ASD (left plots) and control groups (right plots) are shown separately for the MSF (A) and HSF grating conditions (B). For a clearer display of individual data, N80 amplitudes were scaled using z-score values. (C) Best fitting curves of N80 contrast sensitivity responses of ASD and control groups' averaged data. Vertical ranges represent ± 1 SEM.

sensitivity responses obtained from individual curves, separately in the MSF and HSF grating conditions. Figure 2 illustrates the results of the best fitting curves obtained from this analysis. It shows a set of plots relating N80 amplitudes measured over electrode Oz to contrast level. Each dot represents the z-scored individual N80 amplitudes for the MSF (Figure 2A) and HSF grating conditions (Figure 2B) obtained from each group (ASD and controls). Figure 2C shows N80 contrast–response functions to MSF and HSF gratings separately for ASD and control group averaged data. The curves through the data points were

fitted using a linear regression function, with highly reliable correlation coefficients for both ASD ($r^2 = 0.89$ for MSF; $r^2 = 0.9$ for HSF) and control participants ($r^2 = 0.76$ for MSF; $r^2 = 0.92$ for HSF). To assess possible group differences in the N80 contrast sensitivity responses, we compared the slopes of the regression line (index b) evaluated in each ASD and control participant, separately in the MSF and HSF grating conditions.

Statistical analyses indicated that in the MSF grating condition N80 contrast response slopes increased in a more accelerating fashion for the ASD than control group

($t(28) = 2.59, p = 0.015$) but not in the HSF grating condition ($t(28) = 0.67, p = 0.5$). More interestingly, Figure 2C indicates that contrast sensitivity of N80 responses differed between MSF and HSF grating conditions in controls but not in ASD participants. There was no N80 slope difference between the MSF and HSF grating conditions in the ASD group ($t(15) = 0.35, p = 0.7$). In contrast, the slope was significantly steeper in the HSF than in the MSF grating condition in the control group ($t(13) = 2.33, p = 0.037$).

P100 contrast sensitivity responses

As shown in Figure 1, the three spatial frequency contrast gratings elicited a conspicuous P100 VEP component, whose peak amplitude was maximal over electrode Oz. P100 contrast–response function exhibited a distinct behavior along the spatial frequency domain.

For LSF gratings, P100 responses in both ASD and control participants had a rapid contrast gain at low contrasts and rapidly reached a plateau at 32% contrast level. Figure 3 illustrates the best fitting curves in the LSF grating condition obtained from ASD (A) and control (B)

individual contrast functions and from each group averaged data (C). P100 contrast response curves in both groups were best fit with a saturating hyperbolic function using the Naka–Rushton equation. This resulted in highly good fits for ASD ($r^2 > 0.82$) and controls ($r^2 > 0.78$). The half saturation (b) and response saturation (R_{max}) values, derived from individual fitted curves, were then compared between the two groups. These analyses did not yield any significant differences in half saturation values between ASD ($b = 8.13 \pm 1.2$) and control ($b = 8.53 \pm 1.74$) participants ($t(28) = 0.75, ns$). Comparable P100 saturation responses were found in ASD and control participants ($t(28) = 0.19, ns$).

For MSF and HSF gratings, P100 contrast sensitivity curves were fairly linear and were thus accounted for by a linear regression function, with highly reasonable correlation coefficients for ASD ($r^2 > 0.82$ for MSF, $r^2 > 0.85$ for HSF) and control groups' data ($r^2 > 0.83$ for both MSF and HSF). As can be seen in Figure 4, the slope characterizing the incremental increase of P100 response curves was slightly steeper for MSF than for HSF grating. However, there was no significant difference between the slope index values for MSF and HSF conditions in neither group (all paired t -tests < 0.52). In addition, these slopes

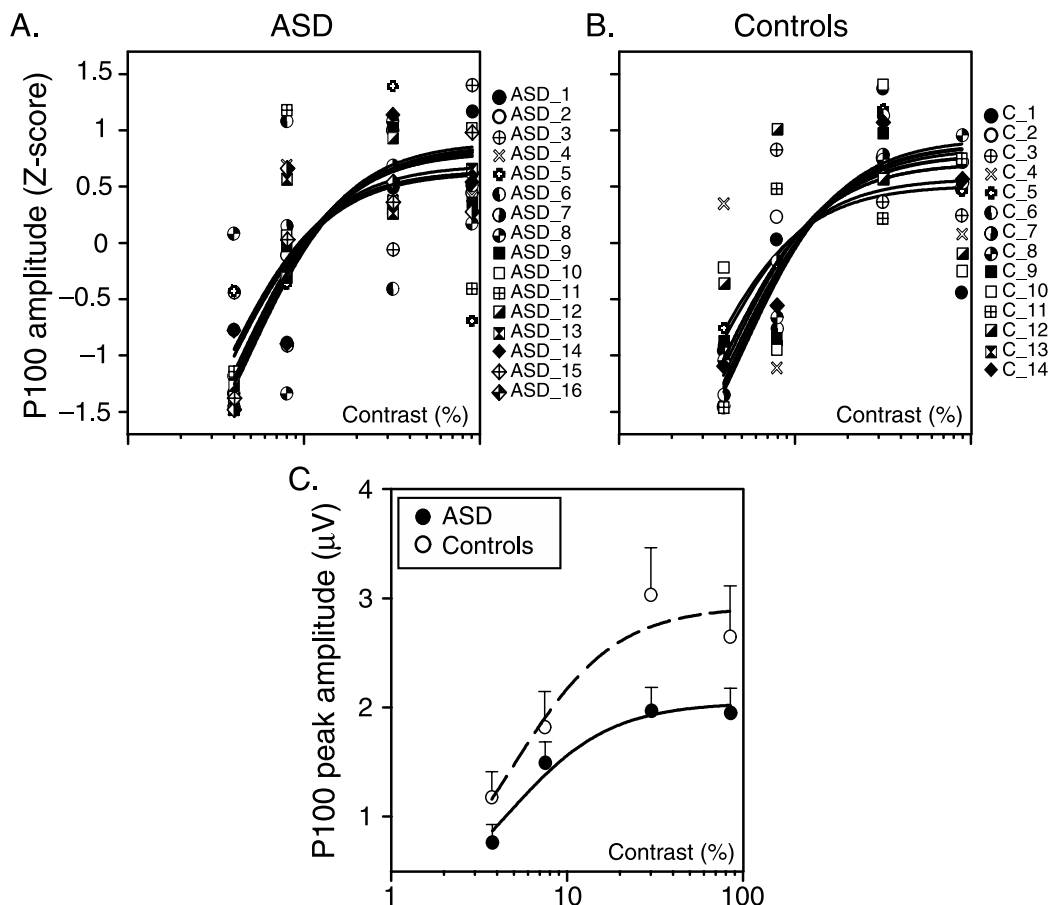


Figure 3. Best fitting curves of P100 contrast sensitivity responses for LSF obtained from each individual data of ASD (A) and control participants (B) and from groups' averaged data (C). Contrast levels in the abscissa are displayed in a logarithmic scale.

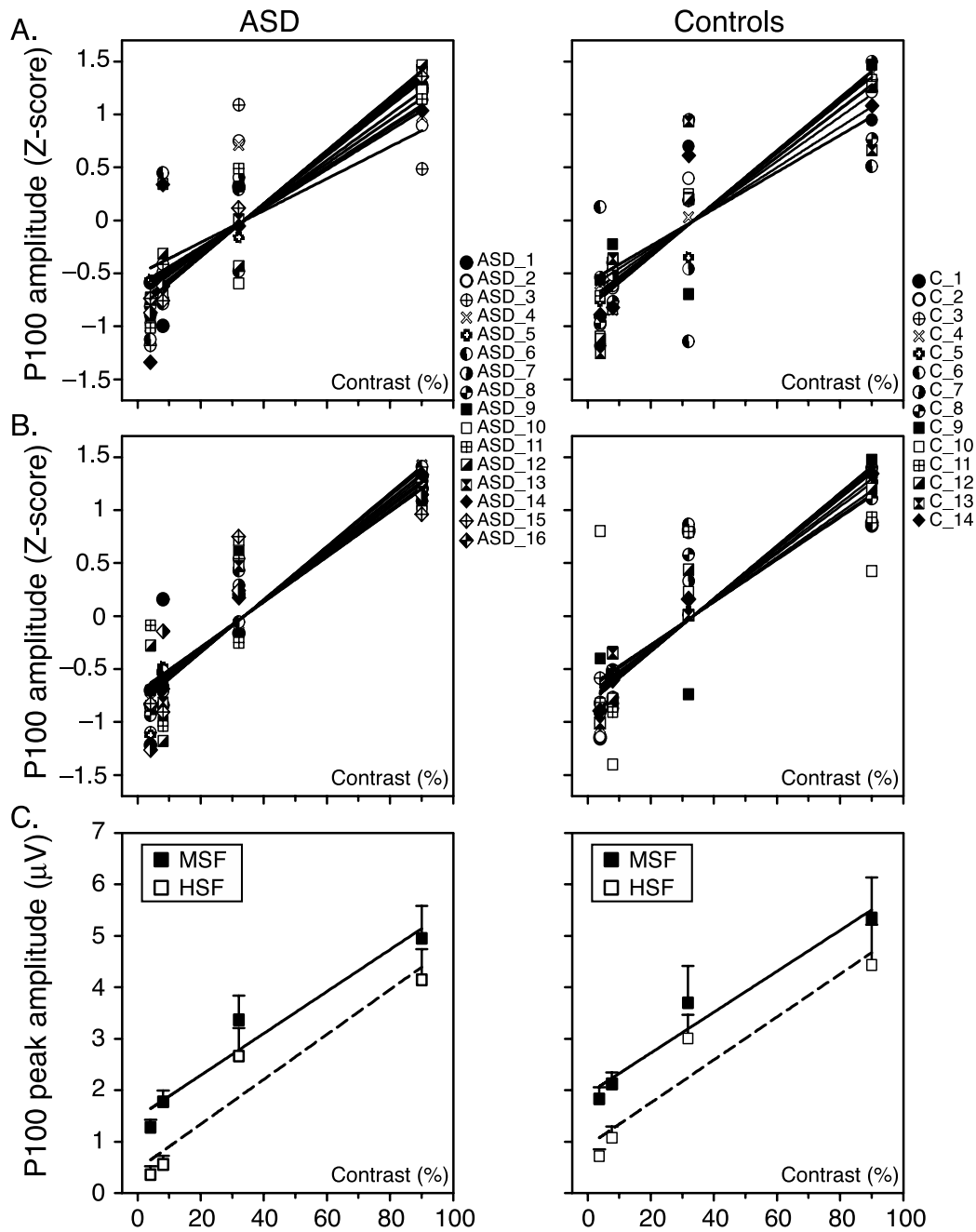


Figure 4. Best fitting curves of P100 contrast sensitivity responses for the MSF (A) and HSF grating conditions (B) obtained from each individual data of ASD (left plots) and control (right plots) groups. (C) P100 contrast sensitivity responses computed with groups' averaged data.

did not differ between the two groups, for both the MSF and HSF grating conditions ($t(28) < 0.61$, *ns*).

Behavioral results

To ascertain that non-visual factors such as differences in attention to the SF gratings do not account for the pattern of results described so far, we compared the accuracy and RTs of the two groups at detecting the rare targets (i.e., horizontal gratings). ASD and control participants performed the detection task at a similar level

of accuracy, $72.6\% \pm 22.4\%$ for ASD and $74.7\% \pm 17.8\%$ for controls ($t(28) = 1.9$, $p > 0.1$), and speed of response, $403.5 \text{ ms} \pm 72.1$ for ASD and $403.1 \text{ ms} \pm 103.5$ for controls ($t(28) = 0.11$, $p > 0.1$).

Discussion

The primary goal of the present study was to characterize the pattern of contrast response tuning of low,

intermediate, and high-filter visual channels in ASD using transient VEPs. We found three main results. First, the pattern of VEP responses to LSF contrast–luminance gratings was similar in ASD and control participants. Second, contrast sensitivity functions of VEP responses to MSF and HSF gratings show striking differences between the ASD and control group. More specifically, while the linear slopes of N80 amplitude versus contrast functions in controls were steeper to HSF than to MSF gratings, N80 contrast–response functions were strikingly identical for HSF and MSF gratings in ASD. Third, N80 peaks to MSF gratings not only saturated in amplitude but also emerged at lower contrast levels (at 32%) in the ASD than in the control group (90%). Taken together, our N80 results suggest a reduced fine tuning of mid and high spatial frequency processing channels in the early cortical visual streams in adults with ASD.

The contrast–response functions of VEP amplitudes to LSF gratings obtained in ASD and control groups display a hyperbolic non-linear type of function, consistent with previous electrophysiological findings in humans (Bach & Ullrich, 1997; Baseler & Sutter, 1997; Ellemberg et al., 2001) and in primates (Kaplan & Shapley, 1986; Shapley & Lennie, 1985). In both groups of participants, P100 to LSF gratings showed a high contrast gain and rapid amplitude saturation at low contrast (~8%). In addition, there were no between-group differences in the half saturation (b) and response saturation (R_{\max}) measures, derived from P100 contrast–response curves. Taken together, our results suggest that the *functional response properties* of low spatial frequency visual channels may be typical in adult participants with ASD.

For mid and high spatial frequency gratings, contrast responses of the recorded VEPs exhibit a low contrast gain with no apparent response saturation as contrast increases (Ellemberg et al., 2001; Kaplan & Shapley, 1986). In both ASD and control participants, N80 and P100 peaks displayed a linear increase in amplitude with increasing contrast level. This amplitude increase did not level off with the highest contrast used (90%). Furthermore, even though VEP contrast–response patterns were overall similar between the two groups of participants, our N80 results revealed some striking processing differences in the early stages of spatial vision between ASD and controls. We found that for the control group, N80 amplitude in response to HSF gratings was larger and its contrast response slope was steeper than that to MSF gratings, probably indexing the differential involvement of visual filter channels for mid and high spatial frequency gratings. A set of six linear, band-pass spatial frequency channels is assumed to operate in parallel in the visual cortex, each of which display a specific contrast–tuning curve. It has been shown that the peak frequencies of these channels are unequally spaced, with estimated peaks at 0.8, 1.7, 2.8, 4.0, 8.0, and 16.0 $\text{c}\cdot\text{deg}^{-1}$. The spatial bandwidths of the lowest spatial frequency channels differ by 2.0 to 2.5 octaves, while 1.25 to 1.6 octaves separate

the high-frequency channels (Graham & Nachmias, 1971; Wilson et al., 1983). The peak frequency of the MSF and HSF gratings used in our study differed by up to 1.5 octaves, a bandwidth spacing that is sufficient to trigger specifically the activity of two distinct spatial channels. Moreover, for the ASD group, N80 peak in response to MSF gratings not only saturated in amplitude but also exhibited identical contrast response slopes as those obtained for high spatial frequency gratings. These findings indicate that the spatial channels tuned to mid- and high-frequency scales behaved alike in ASD, suggesting a reduced fine tuning of visual spatial filters in autistics' primary visual cortex. Taken collectively, the present N80 results do also suggest the intriguing possibility that the visual channels tuned to mid and high spatial frequency inputs are less functionally segregated in ASD.

It is worth mentioning that a similar conclusion has been drawn from two previous electrophysiological studies in children with ASD (Boeschoten et al., 2007a; Milne et al., 2009). The results of Boeschoten et al. (2007a) show decreased differences of VEP responses and of their modeled source activities between low (0.75 $\text{c}\cdot\text{deg}^{-1}$) and high spatial frequency (6 $\text{c}\cdot\text{deg}^{-1}$) square-wave gratings in children with ASD as compared to typical children. Furthermore, Milne et al. (2009) found that the power of gamma and alpha responses was less modulated by the spatial frequency of gabor patches (0.5, 1, 4, and 8 $\text{c}\cdot\text{deg}^{-1}$) in children with ASD than in control children. Overall, these findings suggest reduced neurofunctional specialization of visual channels tuned to a wide range of spatial frequency patterns, from the very coarse to the very fine. The fact that the present study did not find any abnormality in the VEP contrast responses to LSF gratings in adults with ASD does not preclude the possibility that atypicalities in processing low spatial frequency information may be present in children with ASD (cf. McCleery et al., 2007; Milne et al., 2002; Spencer & O'Brien, 2006; Spencer et al., 2000). Further studies are however needed to gain a better understanding of the developmental trajectories of early visual channels in ASD across age.

Finally, how do the present findings resonate with our current knowledge on the superiority of persons with autism to process visual details? It is still generally agreed that the outcome of the early stages of spatial vision constitutes the building blocks of visual perception (Morrison & Schyns, 2001). A dysfunction at this stage might have dramatic impact on the way information is handled at later stages of visual processing. The fact that ASD individuals generally show enhanced processing of details of non-social (Dakin & Frith, 2005) but also social visual materials (Lahaie et al., 2006; for a review, see Jemel et al., 2006) has lead some authors to suggest either a deficit in low spatial filter channels that convey global information (Milne et al., 2002; Spencer et al., 2000) or an overfunctioning of high spatial visual channels that convey local information (Deruelle, Rondan, Gepner, & Tardif, 2004; Mottron et al., 2006). Our current results

support neither of these two accounts. Marked differences between ASD and controls however arose for mid spatial frequency gratings, indicating a similar contrast response range of visual channels processing mid and high spatial frequency information. In other words, our findings do suggest that visual inputs that frequency content falls within $2.8 \text{ c}\cdot\text{deg}^{-1}$ frequency range may be processed in a similar manner as high spatial frequency contents ($8 \text{ c}\cdot\text{deg}^{-1}$) in adults with autism (Boeschoten, Kenemans, van Engeland, & Kemner, 2007b). Such an undifferentiated coding mechanism of neural units tuned to mid and high spatial frequency inputs implies that processing of a large range of stimuli, including faces would be biased towards detection of compounds. It is worth noting that the wavelength of MSF grating used in our study is close to the upper limit of the spatial frequency band ($15 \text{ c}/\text{face width}$ corresponding to $2.2 \text{ c}\cdot\text{deg}^{-1}$) that has been demonstrated to be critical for face recognition (Näsänen, 1999; Parker & Costen, 1999; Tieger & Ganz, 1979).

Conclusions

In this paper, we address the question whether the early cortical visual processes of spatial channels tuned to low, mid, and high spatial frequency inputs in autism show some modified functional properties with respect to typical adults. VEPs recorded to sinusoidal contrast reversal gratings revealed similar response contrast functions for ASD and controls to low and high spatial frequency gratings. Moreover, contrary to the controls' results, VEP contrast sensitivity to mid spatial frequency gratings in ASD was not different from that obtained for high spatial frequency gratings. Our present findings provide evidence for an altered functional segregation of early visual channels, especially those responsible for processing mid-frequency spatial scale. It is thus possible that their tendency to process visual details stems from the fact that a wide range of visual stimuli that fall within the mid-frequency range may be processed using the same mechanisms as those devoted to process high spatial frequency information.

Acknowledgments

This work was made possible by a grant from the Canadian Institutes of Health Research (MOP-82749) awarded to the first author.

Commercial relationships: none.

Corresponding author: Boutheina Jemel.

Email: boutheina.jemel@umontreal.ca.

Address: Research Laboratory in Neuroscience and Cognitive Electrophysiology, Hôpital Rivière des Prairies, 7070 Bld Perras, Montreal (H1E 1A4), Canada.

References

- American Psychiatric Association (2000). *Diagnostic and statistical manual of mental disorders* (4th ed.). Washington, DC: Author.
- Bach, M., & Ullrich, D. (1997). Contrast dependency of motion-onset and pattern-reversal VEPs: Interaction of stimulus type, recording site and response component. *Vision Research*, *37*, 1845–1849. [[PubMed](#)] [[Article](#)]
- Baseler, H. A., & Sutter, E. E. (1997). M and P components of the VEP and their visual field distribution. *Vision Research*, *37*, 675–690. [[PubMed](#)] [[Article](#)]
- Behrmann, M., Avidan, G., Leonard, G. L., Kimchi, R., Luna, B., Humphreys, K., et al. (2006). Configural processing in autism and its relationship to face processing. *Neuropsychologia*, *44*, 110–129. [[PubMed](#)] [[Article](#)]
- Bertone, A., Mottron, L., Jelenic, P., & Faubert, J. (2005). Enhanced and diminished visuo-spatial information processing in autism depends on stimulus complexity. *Brain*, *128*, 2430–2441. [[PubMed](#)] [[Article](#)]
- Boeschoten, M. A., Kenemans, J. L., van Engeland, H., & Kemner, C. (2007a). Abnormal spatial frequency processing in high-functioning children with pervasive developmental disorder (PDD). *Clinical Neurophysiology*, *114*, 1619–1629. [[PubMed](#)]
- Boeschoten, M. A., Kenemans, J. L., van Engeland, H., & Kemner, C. (2007b). Face processing in Pervasive Developmental Disorder (PDD): The roles of expertise and spatial frequency. *Journal of Neural Transmission*, *118*, 2076–2088. [[PubMed](#)]
- Bulens, C., Meerwaldt, J. D., van der Wildt, G. J., & Keemink, C. J. (1988). Spatial contrast sensitivity in clinical neurology. *Clinical Neurology and Neurosurgery*, *90*, 29–34. [[PubMed](#)]
- Butler, P. D., Martinez, A., Foxe, J. J., Kim, D., Zemon, V., Silipo, G., et al. (2007). Subcortical visual dysfunction in schizophrenia drives secondary cortical impairments. *Brain*, *130*, 417–430. [[PubMed](#)] [[Article](#)]
- Campbell, F. W., & Green, D. G. (1965). Optical and retinal factors affecting visual resolution. *The Journal of Physiology*, *181*, 576–593. [[PubMed](#)]
- Campbell, F. W., & Robson, J. G. (1968). Application of Fourier analysis to the visibility of gratings. *The Journal of Physiology*, *197*, 551–556. [[PubMed](#)] [[Article](#)]
- Caron, M.-J., Mottron, L., Berthiaume, C., & Dawson, M. (2006). Cognitive mechanisms, specificity and neural underpinnings of visuospatial peaks in autism. *Brain*, *129*, 1789–1802. [[PubMed](#)] [[Article](#)]

- Dacey, D. M., & Petersen, M. R. (1992). Dendritic field size and morphology of midget and parasol ganglion cells of the human retina. *Proceedings of the National Academy of Sciences of the United States of America*, *89*, 9666–9670. [PubMed] [Article]
- Dakin, S., & Frith, U. (2005). Vagaries of visual perception in autism. *Neuron*, *48*, 497–507. [PubMed]
- Davis, R. A. O., Bockbrader, M. A., Murphy, R. R., Hetrick, W. P., & O'Donnell, B. F. (2006). Subjective perceptual distortions and visual dysfunction in children with autism. *Journal of Autism and Developmental Disorders*, *36*, 199–210. [PubMed]
- de Jonge, M. V., Kemner, C., de Haan, E. H., Coppens, J. E., van den Berg, T. J., & van Engeland, H. (2007). Visual information processing in high-functioning individuals with autism spectrum disorders and their parents. *Neuropsychology*, *21*, 65–73. [PubMed] [Article]
- Deruelle, C., Rondan, C., Gepner, B., & Tardif, C. (2004). Spatial frequency and face processing in children with autism and Asperger syndrome. *Journal of Autism and Developmental Disorders*, *34*, 199–210. [PubMed]
- DeValois, R. L., & DeValois, K. K. (1988). *Spatial vision*. New York: Oxford University Press.
- Ellemberg, D., Hammarrenger, B., Lepore, F., Roy, M.-S., & Guillemot, J.-P. (2001). Contrast dependency of VEPs as a function of spatial frequency: The parvocellular and magnocellular contributions to human VEPs. *Spatial Vision*, *15*, 99–111. [PubMed]
- Fiorentini, A., Pirchio, M., & Spinelli, D. (1980). Scotopic contrast sensitivity in infants evaluated by evoked potentials. *Investigative Ophthalmology & Visual Science*, *19*, 950–955. [PubMed]
- Graham, N., & Nachmias, J. (1971). Detection of grating patterns containing two spatial frequencies: A comparison of single-channel and multiple channel-models. *Vision Research*, *11*, 251–259. [PubMed]
- Happé, F. (1999). Autism: Cognitive deficit or cognitive style? *Trends in Cognitive Sciences*, *3*, 216–222. [PubMed] [Article]
- Jemel, B., Mottron, L., & Dawson, M. (2006). Impaired face processing in autism: Fact or artefact? *Journal of Autism and Developmental Disorders*, *36*, 91–106. [PubMed]
- Jolliffe, T., & Baron-Cohen, S. (1997). Are people with autism and Asperger syndrome faster than normal on the embedded figures test? *Journal of Child Psychology and Psychiatry*, *38*, 527–534. [PubMed]
- Kaplan, E., & Shapley, R. M. (1986). The primate retina contains two types of ganglion cells, with high and low contrast sensitivity. *Proceedings of the National Academy of Sciences of the United States of America*, *83*, 2755–2757. [PubMed] [Article]
- Klitorner, A., Crewther, D. P., & Crewther, S. G. (1997). Separate magnocellular and parvocellular contributions from temporal analysis of the multifocal VEP. *Vision Research*, *37*, 2161–2169. [PubMed] [Article]
- Lahaie, A., Mottron, L., Arguin, M., Berthiaume, C., Jemel, B., & Saumier, D. (2006). An investigation of configural and part-based face processing in high-functioning autism. *Neuropsychology*, *20*, 30–41.
- Lord, C., Risi, S., Lambrecht, L., Cook, E. H., Lenventhal, B. L., DiLavore, P. C., et al. (2000). The autism diagnostic observation schedule-generic: A standard measure of social and communication deficits associated with the spectrum of autism. *Journal of Autism and Developmental Disorders*, *30*, 205–223. [PubMed]
- Lord, C., Rutter, M., & Le Couteur, A. (1994). Autism diagnostic interview-revised: A revised version of a diagnostic interview for caregivers of individuals with possible pervasive developmental disorders. *Journal of Autism and Developmental Disorders*, *24*, 659–685. [PubMed]
- McCleery, J. P., Allman, E., Carver, L., & Dobkins, K. R. (2007). Abnormal magnocellular pathway visual processing in infants at risk for autism. *Biological Psychiatry*, *62*, 1007–1014. [PubMed]
- McKee, S. P., Levi, D. M., & Movshon, J. A. (2003). The pattern of visual deficits in amblyopia. *Journal of Vision*, *3*(5):5, 380–405, <http://www.journalofvision.org/content/3/5/5>, doi:10.1167/3.5.5. [PubMed] [Article]
- Michelson, A. (1927). *Studies in optics*. Chicago: University of Chicago Press.
- Mihaylova, M., Stomonyakov, V., & Vassilev, A. (1999). Peripheral and central delay in processing high spatial frequencies: Reaction time and VEP latency studies. *Vision Research*, *39*, 699–705. [PubMed] [Article]
- Milne, E., Scope, A., Pascalis, O., Buckley, D., & Makeig, S. (2009). Independent component analysis reveals atypical electroencephalographic activity during visual perception in individuals with autism. *Biological Psychiatry*, *65*, 22–30. [PubMed]
- Milne, E., Swettenham, J., Hansen, P., Campbell, R., Jeffries, H., & Plaisted, K. (2002). High motion coherence thresholds in children with autism. *Journal of Child Psychology and Psychiatry*, *43*, 255–263. [PubMed] [Article]
- Morrison, D. J., & Schyns, P. G. (2001). Usage of spatial scales for the categorization of faces, objects, and scenes. *Psychonomic Bulletin and Review*, *8*, 454–469. [PubMed]
- Mottron, L., Dawson, M., Soulières, I., Hubert, B., & Burack, J. (2006). Enhanced perceptual functioning in

- autism: An update, and eight principles of autistic perception. *Journal of Autism and Developmental Disorders*, *36*, 27–43. [PubMed]
- Movson, J. A., & Kiorpes, L. (1988). Analysis of the development of spatial contrast sensitivity in monkey and human infants. *Journal of the Optical Society of America A, Optics and Image Science*, *5*, 2166–2172. [PubMed]
- Naka, K. I., & Rushton, W. A. (1966). S-potentials from colour units in the retina of fish (Cyprinidae). *The Journal of Physiology*, *185*, 536–555. [PubMed] [Article]
- Näsänen, R. (1999). Spatial frequency bandwidth used in the recognition of facial images. *Vision Research*, *39*, 3824–3833. [PubMed] [Article]
- Nassi, J. J., & Callaway, E. M. (2009). Parallel processing strategies of the primate visual system. *Nature Reviews. Neuroscience*, *10*, 360–372. [PubMed] [Article]
- Nelson, J. I., & Seiple, W. H. (1992). Human VEP contrast modulation sensitivity: Separation of magnocellular and parvocellular components. *Electroencephalography and Clinical Neurophysiology*, *84*, 1–12. [PubMed]
- Norcia, A. M., & Tyler, C. W. (1985). Spatial frequency sweep VEP: Visual acuity during the first year of life. *Vision Research*, *25*, 1399–1408. [PubMed] [Article]
- Nunez, P. L. (1981). *Electric fields of the brain*. New York: Oxford University Press.
- O’Riordan, M., Plaisted, K., Driver, J., & Baron-Cohen, S. (2001). Superior visual search in autism. *Journal of Experimental Psychology: Human Perception and Performance*, *27*, 719–730. [PubMed] [Article]
- Pantle, A., & Sekuler, R. (1968). Size detecting mechanisms in human vision. *Science*, *162*, 1146–1148. [PubMed]
- Parker, D., & Costen, N. (1999). One extreme or the other, or perhaps the Golden Mean: Issues of spatial resolution in face processing. *Current Psychology*, *18*, 118–127.
- Plant, G. T., Zimmern, R. L., & Durden, K. (1983). Transient visually evoked potentials to the pattern reversal and onset of sinusoidal gratings. *Electroencephalography and Clinical Neurophysiology*, *56*, 147–158. [PubMed]
- Regan, D. (1989). *Human brain electrophysiology*. New York: Elsevier.
- Rinehart, N. J., Bradshaw, J. L., Moss, S. A., Breerton, A. V., & Tonge, B. J. (2000). Atypical interference of local detail on global processing in high-functioning autism and Asperger’s disorder. *Journal of Child Psychology and Psychiatry*, *41*, 769–778. [PubMed]
- Rudvin, I., Valberg, A., & Kilavik, B. E. (2000). Visual evoked potentials and magnocellular and parvocellular segregation. *Vision Neuroscience*, *17*, 579–590. [PubMed]
- Sekuler, R., & Hutman, L. P. (1980). Spatial vision and aging: I. Contrast sensitivity. *Journal of Gerontology*, *35*, 692–699. [PubMed]
- Shah, A., & Frith, U. (1983). An islet of ability in autistic children: A research note. *Journal of Child Psychology and Psychiatry*, *24*, 613–620. [PubMed]
- Shah, A., & Frith, U. (1993). Why do autistic individuals show superior performance on the block design task? *Journal of Child Psychology and Psychiatry*, *34*, 1351–1364. [PubMed]
- Shapley, R. (1990). Visual sensitivity and parallel retinocortical channels. *Annual Review of Psychology*, *41*, 635–658. [PubMed] [Article]
- Shapley, R., & Enroth-Cugell, C. (1984). Visual adaptation and retinal gain controls. In N. Osborne & G. Chader (Eds.), *Progress in retinal research* (vol. 3, pp. 263–346). London: Pergamon.
- Shapley, R., & Lennie, P. (1985). Spatial frequency analysis in the visual system. *Annual Review of Neuroscience*, *8*, 547–583. [PubMed] [Article]
- Sharbrough, F., Chatrian, G. E., Lesser, R. P., Lüders, H., Nuwer, M., & Picton, T. W. (1991). American electroencephalographic society guidelines for standard electrode position nomenclature. *Journal of Clinical Neurophysiology*, *8*, 200–202.
- Souza, G. S., Gomes, B. D., Saito, C. A., da Silva Filho, M., & Silveira, L. C. (2007). Spatial luminance contrast sensitivity measured with transient VEP: Comparison with psychophysics and evidence of multiple mechanisms. *Investigative Ophthalmology & Visual Science*, *48*, 3396–3404. [PubMed] [Article]
- Spencer, J., O’Brien, J., Riggs, K., Braddick, O., Atkinson, J., & Wattam-Bell, J. (2000). Motion processing in autism: evidence for a dorsal stream deficiency. *Neuroreport*, *11*, 2765–2767. [PubMed]
- Spencer, J. V., & O’Brien, J. M. (2006). Visual form-processing deficits in autism. *Perception*, *35*, 1047–1055. [PubMed]
- Tieger, T., & Ganz, L. (1979). Recognition of faces in the presence of two-dimensional sinusoidal masks. *Perception & Psychophysics*, *26*, 163–167.
- Vassilev, A., Mihaylova, M., & Bonnet, C. (2002). On the delay in processing high spatial frequency visual information: Reaction time and VEP latency study of the effect of local intensity of stimulation. *Vision Research*, *42*, 851–864. [PubMed] [Article]
- Vassilev, A., Stomonyakov, V., & Manahilov, V. (1994). Spatial-frequency specific contrast gain and flicker masking of human transient VEP. *Vision Research*, *34*, 863–872. [PubMed] [Article]

- Volkmar, F., Lord, C., Bailey, A., Schultz, R. T., & Klin, A. (2004). Autism and pervasive developmental disorders. *Journal of Child Psychology and Psychiatry*, *45*, 135–170. [[PubMed](#)]
- Wang, L., Mottron, L., Peng, D., Berthiaume, C., & Dawson, M. (2007). Local bias and local-to-global interference without global deficit: A robust finding in autism under various conditions of attention, exposure time, and visual angle. *Cognitive Neuropsychology*, *24*, 550–574. [[PubMed](#)]
- Wechsler, D. (1997). *Wechsler Intelligence Scale* (3rd ed.). San Antonio, TX: The Psychological Corporation.
- Wilson, H. R., McFarlane, D. K., & Phillips, G. C. (1983). Spatial tuning of orientation selective units estimated by oblique masking. *Vision Research*, *23*, 873–882. [[PubMed](#)] [[Article](#)]
- Wilson, H. R., & Wilkinson, F. (2004). Spatial channels in vision and spatial pooling. In L. M. Chalupa & J. S. Werner (Eds.), *The visual neuroscience* (vol. 2, pp. 1060–1068). Cambridge: MIT Press.